Antichiral order and spin reorientation transitions of triangle-based antiferromagnets

Leon Balents

Phys. Rev. B **106**, L020403 — Published 22 July 2022

DOI: 10.1103/PhysRevB.106.L020403

Anti-chiral order and spin reorientation transitions of triangle-based antiferromagnets

Leon Balents[1,2]
(1)Kavli Institute for Theoretical Physics, University of California, Santa Barbara, California 93106-4030, USA
(2) Canadian Institute for Advanced Research, Toronto, Ontario, Canada
(Dated: June 22, 2022)

We show that triangle-based antiferromagnets with "anti-chiral" order display a non-trivial dependence of the spin orientation with an in-plane field. The spins evolve from rotating in the opposite sense to the field at very low fields to rotating in the same sense as the field above some critical field scale. In the latter regime the system displays first order transitions at which the spin angles jump, and these first order lines terminate in critical points in the Ising universality class. Application to Mn_3Sn is discussed.

The elementary unit of a triangle of spins is often considered the building block of frustrated magnetism. Three spins on such a triangle with antiferromagnetic Heisenberg interactions enjoy, in the classical limit, an O(3) rotational degeneracy of ground states in which the spins lie in a plane at 120 degree angles to one another. When a field is applied, the degeneracy enlarges from this symmetry-mandated one to an accidental degeneracy which includes both coplanar and non-coplanar states. When such triangles are assembled into the canonical triangular lattice,[1] thermal and quantum fluctuations are known to break this degeneracy in favor of the coplanar ones, a phenomena known as "order by disorder"[2]. Larger degeneracies are found when the triangles are more weakly connected, as in the famous kagomé lattice. There the Heisenberg degeneracy becomes extensive, and ordering is strongly suppressed. Commonly in real materials, weak symmetry breaking effects such as Dzyaloshinskii-Moriya (DM) coupling[3] and single-ion anisotropy (SIA) provide another degeneracy breaking mechanism leading to a selection of three-sublattice ordered states.

In this paper, we study a very common situation of three-sublattice order based on triangles in which the Heisenberg O(3) symmetry of the Hamiltonian is weakly broken by DM and SIA in favor of coplanar order in zero applied field.. We adopt a symmetry-based approach based on order parameters, which is more universal than microscopic models of specific exchange interactions, but which incorporates a hierarchy of coupling strengths. In particular, we assume that Heisenberg exchange J is the largest scale, followed by DM with strength D and SIA of strength K, i.e. $J \gg D \gg K$. This is inspired by the breathing kagomé lattice materials Mn_3Sn and Mn_3Ge[4–10], but is very typical for third row transition metal magnets. We focus on the anti-chiral state (selected for $D > 0$, see Eq. (5)), in which, proceeding clockwise around the triangle, spins rotate counter-clockwise (Fig. 1). Spins in the anti-chiral state are nearly free to rotate globally (see below). From this perspective, we consider the evolution of the spin configurations in an applied field, and in particular how the spins rotate when the field is rotated within the XY plane favored by DM coupling. We show that there is an emergent low magnetic field scale H^* separating two distinct behaviors. When the field is much smaller than H^*, the angle of a single spin within the plane rotates in the opposite sense as the field, i.e. if the field is oriented at an angle θ in this plane, each spin rotates with angle $\phi_n = \phi_n^{(0)} - \theta$, where $\phi_n^{(0)}$ is an offset for each sublattice n. Conversely, when the field is much larger than H^*, the spins rotate in sync with the field, i.e. $\phi_n = \phi_n^{(0)} + \theta$. These competing tendencies result in abrupt and discontinuous changes in the spin configurations, which form lines of first order transitions in the plane of the magnetic field, terminating at second order Ising critical points (see Fig. 3). We argue that features recently observed in sensitive measurements of the angular dependence of magnetization and torque in Mn_3Sn[5] are precursors of these transitions, and that the transitions should be observable in higher magnetic fields. The theory should also be applicable to other kagomé magnets with anti-chiral order, of which there are several examples[11–14].

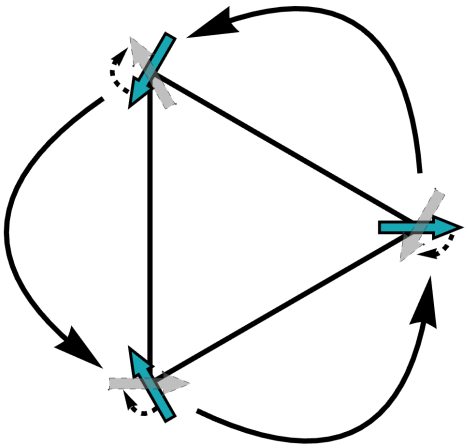

FIG. 1. Illustration of the behavior of anti-chiral spins under rotations. A counter-clockwise rigid rotation of the triangle by 120 degrees, indicated by the solid arrows, rotates the spins from their initial state (shown in blue) to a new state, shown in gray. This is equivalent to a clockwise rotation of the spins by 120 degrees (indicated by the smaller dashed arrows) in place.

Symmetry and order parameters: We begin by present-

ing a derivation of the free energy as a function of spin angle based on symmetry and the hierarchy of energy scales. We assume at the outset that we have a magnetic system whose ordered structure is fully specified by giving the orientation of a set of three spins on an elementary triangle. We further assume that the dominant interactions between these three spins are antiferromagnetic and isotropic,

$$H_0 = J\left(\boldsymbol{S}_0\cdot\boldsymbol{S}_1+\boldsymbol{S}_1\cdot\boldsymbol{S}_2+\boldsymbol{S}_2\cdot\boldsymbol{S}_0\right), \tag{1}$$

with $J>0$. This favors an ordered state in which the three spins sum to zero, and have equal magnitudes:

$$\langle\boldsymbol{S}_n\rangle = \mathrm{Re}\left[\boldsymbol{d}\,e^{\frac{2\pi i n}{3}}\right], \tag{2}$$

where the angular brackets denote the usual equilibrium thermal expectation value, and $\boldsymbol{d}$ is a complex vector satisfying

$$\boldsymbol{d}\cdot\boldsymbol{d}=0. \tag{3}$$

The last relation implies that the magnitude $|\langle\boldsymbol{S}_n\rangle|$ is independent of $n=0,1,2$. This is not a requirement, but would be expected at low temperature classically.

Note that although at a microscopic model level the spins may be taken as either quantum operators or fixed length vectors (classically), the order parameter $\boldsymbol{d}$ as defined is always a classical variable, which enables a simple analytic treatment, which is valid regardless of the microscopic formulation.

In general, the order parameter can also be written in terms of two orthogonal real vectors of equal magnitude, $\boldsymbol{d}=\boldsymbol{u}+i\boldsymbol{v}$, where Eq. (3) implies $|\boldsymbol{u}|^2=|\boldsymbol{v}|^2$, $\boldsymbol{u}\cdot\boldsymbol{v}=0$. These two vectors $\boldsymbol{u},\boldsymbol{v}$ define a plane in which the spins lie. From this one can define a third vector normal to the plane, $\boldsymbol{w}=\boldsymbol{u}\times\boldsymbol{v}=\frac{1}{2}\mathrm{Im}\left(\boldsymbol{d}^*\times\boldsymbol{d}\right)$.

In the following, we use the assumption that perturbations from the Heisenberg limit, i.e. DM, SIA, and applied field, are all small compared to J. Then deviations from the above form are small and more importantly they can be considered to be induced by the perturbations. In the effective field theory (or Landau) sense such deviations correspond to massive modes or subdominant order parameters, and can be integrated out order by order in the perturbations. This allows one to work with an effective free energy which is a function of $\boldsymbol{d}$ only (satisfying Eq. (3)), but in which the strength of perturbations may enter non-linearly.

We construct this free energy based on symmetry and the hierarchy of interactions. First, consider the symmetries in the isotropic limit where $D=K=0$, i.e. with the Hamiltonian in Eq. (1). There is in this case a global SO(3) symmetry under $\boldsymbol{S}_n\to\mathsf{O}\boldsymbol{S}_n$, where O is an arbitrary SO(3) matrix. From Eq. (2), this takes $\boldsymbol{d}\to\mathsf{O}\boldsymbol{d}$. Second, Eq. (1) has full S_3 symmetry under arbitrary permutations of the three spins. It is convenient to regard the permutation symmetry as generated by a $\mathbb{Z}_3$ cyclic permutation which takes $\boldsymbol{S}_n\to\boldsymbol{S}_{n+1}$ and a $\mathbb{Z}_2$ permutation which exchanges $\boldsymbol{S}_1\leftrightarrow\boldsymbol{S}_2$. Under these two operations, respectively, we have $\boldsymbol{d}\to e^{2\pi i/3}\boldsymbol{d}$ and $\boldsymbol{d}\to\boldsymbol{d}^*$.

In zero magnetic field, the only non-zero invariant (using Eq. (3)) under all these symmetries is $\boldsymbol{d}^*\cdot\boldsymbol{d}$, so the zero field free energy in the isotropic limit is a function of this quantity alone. This dependence can be regarded as simply fixing the overall magnitude of the order parameter, $\boldsymbol{d}^*\cdot\boldsymbol{d}=2n_0^2$, where n_0 is the size of a local moment. While this may shift slightly as anisotropy and field are turned on, the effects can be absorbed in other terms, and we can treat it, following the Landau logic, as fixed.

With this understanding, we now introduce the magnetic field $\boldsymbol{h}$ on the isotropic spins. It transforms in the same was $\boldsymbol{d}$ under global SO(3) rotations, and is invariant under all the permutations. Consequently, we find that the purely field-induced terms in the free energy are of the form

$$F_h^{\mathrm{iso}} = c_1|\boldsymbol{h}\cdot\boldsymbol{d}|^2+c_2\mathrm{Re}\left[\left(\boldsymbol{h}\cdot\boldsymbol{d}\right)^3\right]+O(h^4). \tag{4}$$

As is typical for an antiferromagnet, there is no linear coupling of the field to the order parameter, but in this case both quadratic and cubic terms occur[15, 16].

The physical meaning of these terms is as follows. The leading quadratic term selects configurations in which the spins lie in a plane either normal to or containing the field, for $c_1>0$ and $c_1<0$, respectively. Note that the form in Eq. (2) only defines the antiferromagnetic components of the spins (the primary order parameter), and not the field-induced uniform moment. For the semi-classical Heisenberg antiferromagnet on the triangular lattice, the two types of orderings are classically degenerate (i.e. at $1/S=T=0$), but it is known that the coplanar configurations are favored by both thermal and quantum fluctuations, which selects $c_1<0$ ($c_1\sim-1/(JS)$ at $T=0$)[17]. The cubic term selects an orientation of the spins within this plane: when the sign of c_2 is positive (negative), one of the three spins lies anti-parallel (parallel) to the field. According to Ref.17, for the triangular lattice the preferred configuration of the former type, and $c_2>0$ ($c_2\sim1/(J^2S)$ in at $T=0$). The same signs are found for the classical kagomé lattice at non-zero temperature due to thermal fluctuations (though the estimates differ quantitatively due to the higher degeneracy of the kagomé case)[18].

Now consider the effects of DM and SIA, of the microscopic form

$$H' = \sum_n\left[D\hat{\boldsymbol{z}}\cdot\boldsymbol{S}_n\times\boldsymbol{S}_{n+1}-K\left(\hat{\boldsymbol{e}}_n\cdot\boldsymbol{S}_n\right)^2\right], \tag{5}$$

where $\hat{\boldsymbol{e}}_n=(\cos(\frac{2\pi n}{3}),\sin(\frac{2\pi n}{3}),0)$. These additional terms lower the symmetry as follows. The DM interaction D maintains a global SO(2)/U(1) subgroup of SO(3) under rotations about the $\hat{\boldsymbol{z}}$ axis, under the $\mathbb{Z}_3$ cyclic permutation of the spins, and under the spin-orbit coupled C_2 symmetry in which the $\mathbb{Z}_2$ spin permutation discussed

earlier is combined with the corresponding rotation in spin space:

$$C_2: \qquad \boldsymbol{S}_0 \to \mathsf{O}_2 \boldsymbol{S}_0 \qquad \boldsymbol{S}_{1/2} \to \mathsf{O}_2 \boldsymbol{S}_{2/1}, \tag{6}$$

where $\mathsf{O}_2 = \mathrm{diag}(1,-1,-1)$. With the SIA term K, the symmetry is further reduced, so that the global SO(2) and $\mathbb{Z}_3$ operations are collapsed to a single C_3 combined rotation

$$C_3: \qquad \boldsymbol{S}_n \to \mathsf{O}_3 \boldsymbol{S}_{n+1}, \tag{7}$$

where O_3 is the appropriate rotation matrix.[19]

To incorporate the symmetry-lowering effects, it is convenient to adopt a new basis

$$d_\pm = \frac{1}{2}(d_x \pm i d_y), \tag{8}$$

and trade $\boldsymbol{d}$ for d_+, d_- and d_z. Note that because $\boldsymbol{d}$ is complex, d_+ is not the conjugate of d_- and is an independent complex field. The symmetry operations in the new basis become

$$\begin{aligned}
SO(2): d_+ &\to e^{i\vartheta} d_+, & d_- &\to e^{-i\vartheta} d_-, & d_z &\to d_z,\\
\mathbb{Z}_3: d_+ &\to e^{2\pi i/3} d_+, & d_- &\to e^{2\pi i/3} d_-, & d_z &\to e^{2\pi i/3} d_z,\\
\mathbb{Z}_2: d_+ &\to d_-^*, & d_- &\to d_+^*, & d_z &\to d_z^*,\\
C_3: d_+ &\to e^{4\pi i/3} d_+, & d_- &\to d_-, & d_z &\to e^{2\pi i/3} d_z,\\
C_2: d_+ &\to d_+^*, & d_- &\to d_-^*, & d_z &\to -d_z^*,\\
\mathcal{T}: d_+ &\to -d_+, & d_- &\to -d_-, & d_z &\to -d_z.
\end{aligned} \tag{9}$$

To summarize, the DM term is invariant under $SO(2)$, $\mathbb{Z}_3$, C_2 and $\mathcal{T}$. The K term is invariant under C_3,C_2 and $\mathcal{T}$. So the first three lines above are approximate symmetries while the final three are exact. It is also useful to note that under $\mathbb{Z}_2$, $D \to -D$ (but $\mathbb{Z}_2$ does not act simply upon K).

Using the above symmetries, and using the constraint Eq. (3) and the condition that $\boldsymbol{d}^* \cdot \boldsymbol{d} = 2n_0^2$, the most general, non-constant free energy terms at zero field and quadratic in $\boldsymbol{d}$ are

$$\begin{aligned}
F_2 =& s_1 \left(d_+^* d_+ - d_-^* d_-\right)\\
&+ s_2 \left(d_z^* d_z - 2 d_+^* d_+ - 2 d_-^* d_-\right) + s_3 \mathrm{Re}\left(d_-^2\right).
\end{aligned} \tag{10}$$

A naïve calculation, simply inserting Eq. (2) in Eq. (5), shows that $s_1 \sim -D$, $s_3 \sim -K$, while $s_2 \sim K$, while an additional contribution $\Delta s_2 \sim D^2/J$ is expected to arise at second order in the DM coupling (it must be odd in D because under $\mathbb{Z}_2$ $D \to -D$ but s_2 is invariant). In both cases $s_2, s_3 \ll |s_1|$.

Here we are interested in $D > 0$ which implies $s_1 < 0$ which favors $d_- = d_z = 0$ and $|d_+| = n_0$. This is the anti-chiral state. Then the s_2 term is constant and the s_3 term vanishes. Note that the phase of d_+ is arbitrary at this level, reflecting the fact that the rotation of the spins is in the opposite sense to the rotation of the local easy axes, so that the two are incompatible. If by contrast we take $D < 0$, the chiral state with $d_+ = d_z = 0$ is stabilized and $|d_-| = n_0$. Then the s_3 term is non-zero and in fact fixes the phase of d_-, which means the spins are not free to rotate in the chiral state.

For the anti-chiral state, the complete freedom to rotate the phase is an artifact of the truncation of Eq. (10) to second order in $\boldsymbol{d}$. A non-trivial invariant fixing the phase of d_+ arises at sixth order:

$$f_6 = \lambda \mathrm{Re}\left(d_+^6\right). \tag{11}$$

We expect that $\lambda \sim K^3/J$ (because it is sixth order in d_+, and hence in spin expectation values, while the K term is quadratic in spins) as was verified by calculations for Mn_3Sn[20], and therefore is extremely small and often negligible.

Now consider the terms involving the magnetic field. Similarly to Eq. (8), define

$$h_\pm = h_x \pm i h_y. \tag{12}$$

Note that $h_\pm^* = h_\mp$ (unlike for $d_\pm$), so it is sufficient to list the properties of h_+ and h_z. Under the various transformations, we have

$$C_3: h_+ \to e^{2\pi i/3} h_+, \qquad h_z \to h_z, \tag{13}$$
$$C_2: h_+ \to h_+^* = h_-, \qquad h_z \to -h_z, \tag{14}$$
$$\mathcal{T}: h_+ \to -h_+, \qquad h_z \to -h_z. \tag{15}$$

Comparing now Eq. (9) and Eq. (13), we can find invariants involving the field and d_μ. To linear order in the field, we find

$$f_{h,1} = g_1 \mathrm{Re}\left(h_+ d_+\right) + g_2\, h_z \mathrm{Im}\left(d_-\right). \tag{16}$$

In Mn_3Sn, where the order is anti-chiral, $d_- = 0$ and only the g_1 term is active. It is order of $g_1 \sim K/J$[20], because it requires non-zero K to break the SO(2) symmetry. We see that the linear coupling to the field multiplies h_+ and d_+, which favors rotating these complex numbers with opposite phases. This expresses the surprising phenomena that each spin in the anti-chiral case at small fields actually rotates in the opposite sense as the applied field! The g_1 term can be understood physically from the picture in Fig. 1: the net effect of a rigid counter-clockwise C_3 rotation of the anti-chiral triangle is the same as rotating the spins in place by a clockwise C_3 rotation.

Note that this effect contradicts the behavior in the isotropic system, which is dictated by the cubic coupling in Eq. (4), and favors rotating each spin in sync with the field. The opposite tendencies lead to a transition as a function of field strength.

To unveil it more cleanly, we focus now on the case in which only d_+ is assumed non-zero, and the magnetic field is in the plane, and write the free energy as a series in d_+ and the field only. We furthermore assume that the higher order terms in field are dominated by the ones

already present in Eq. (4), and simply express those in the case where $d_z = d_- = 0$ in terms of d_+. We find in this case $\boldsymbol{h}\cdot\boldsymbol{d} = 1/2 h_- d_+$ which leads to

$$f_+ = \lambda \,\mathrm{Re}\,\left(d_+^6\right) + g_1 \mathrm{Re}\,(h_+ d_+) + \frac{c_1}{4}|h_+|^2|d_+|^2 + \frac{c_2}{8}\mathrm{Re}\left((h_- d_+)^3\right). \quad (17)$$

Eq. (17) is not the most general free energy allowed by symmetry, but rather the minimal one which includes the largest terms which break all approximate symmetries both at zero and non-zero fields. In particular, λ and g_1 are the leading order (in K) terms that break SO(2) symmetry at zero field and non-zero fields, respectively, as seen from e.g. Ref.[20].

To analyze Eq. (17), we change to angular coordinates, $h_+ = he^{i\theta}$ and $d_+ = de^{i\phi}$. It becomes, up to a constant,

$$f_+ = -w\cos 6\phi - uh\cos(\phi+\theta) - vh^3\cos 3(\phi-\theta), \quad (18)$$

where

$$w = -\lambda d^6, \qquad u = -g_1 d, \qquad v = -c_2 d^3/8. \quad (19)$$

Angular analysis and phase transitions: Eq. (18) is the general result for the angle-dependent free energy of the anti-chiral state. We now show that it exhibits the phase transitions described in the introduction. Without loss

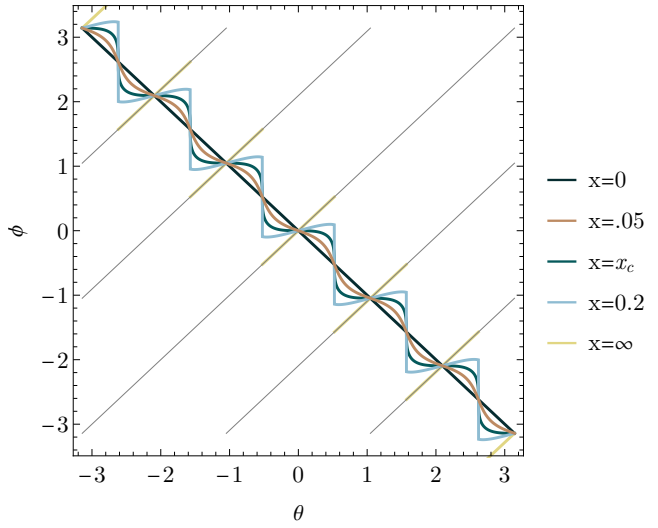

FIG. 2. Spin angle ϕ versus field angle θ for various values of x. The thin gray lines show the 3 degenerate branches at $x=\infty$, while piecewise linear function labeled $x=\infty$ is the one selected at asymptotically large but finite x.

of generality, we take $u, v, w > 0$. Using the aforementioned estimates $w \sim K^3/J^2$,$u \sim K/J$ and $v \sim D/J^3$, we establish the condition $w \ll \sqrt{u^3/v}$, under which w can be neglected in the field regime $h \gg w/u$. We henceforth assume this condition and take $w = 0$. Then the order parameter angle ϕ is determined just by minimizing the final two terms in Eq. (18). So we may write $f_+ = uhg(\phi,\theta)$, with

$$g(\phi,\theta) = -\cos(\phi+\theta) - x\cos 3(\phi-\theta), \quad (20)$$

where $x = \sqrt{v/u}h^2 > 0$. The optimal spin angle $\phi(\theta, x)$ is determined from minimizing g at fixed field angle θ and x. It is instructive to analyze the two limits $x = 0$ and $x = \infty$. At $x = 0$, g is clearly minimized by $\phi = -\theta$. At $x = \infty$, there are three degenerate mnima with $\phi = \theta + 2\pi k/3$, with $k = 0, 1, 2$. One observes that the spin angles winds in the opposite sense in the two extreme limits. The degeneracy in the large x limit is resolved by selecting the branch (k) which minimizes the first term in Eq. (20). This leads to jumps in k (and hence ϕ) as a function of θ, which occur when $\theta = \pi/6 + \pi m/3$, with integer m, as shown in Fig. 2. Away from the two extreme limits, the curve $\phi(\theta)$ evolves, but the discontinuities persist for large x, while they are absence for small x. A transition occurs for $x = x_c$, where the the discontinuities first appear.

To clarify the critical points, we define $\psi = \phi + \theta$, and let $\theta = \pi/6 + \omega$, so that $\omega = 0$ defines the location of one of the discontinuities for $x > x_c$. Some algebra gives

$$\tilde{g}(\psi,\omega) = g(\psi - \tfrac{\pi}{6} - \omega, \theta) = -\cos\psi + x\cos 6\omega\cos 3\psi + x\sin 6\omega\sin 3\psi. \quad (21)$$

We see that at $\omega = 0$, $\tilde{g}(\psi, 0)$ is an even function of ψ. In fact, the even-ness of this function reflects a symmetry $\phi \to \pi/3 - \phi$, which is a C_2 symmetry of the Hamiltonian when the field angle $\theta = \pi/6$. Hence $\tilde{g}(\psi,\omega)$ can be regarded as a Landau function, with a minima at $\psi = 0$ for $x < x_c = 1/9$, which bifurcates for $x > x_c$ into two degenerate minima at $\psi = \pm\psi_0$. This is an Ising phase transition. Note that for Mn_3Sn, the Ising symmetry along these lines can be traced to a symmetry under a C_2 rotation about the axis of the magnetic field, when the field is aligned to these crystalline axes. The deviation ω of the field angle plays the role of a symmetry-breaking field on the Ising order parameter, and the discontinuities in θ are analogous to the first order transition that occurs within the ordered phase of the Ising model on changing the sign of the field. This analysis determines a critical field $h_c = \frac{1}{3}\sqrt{\frac{u}{v}}$. Following the analogy with the Ising model, one observes within this mean field picture that at the critical field, the angle $\psi \sim -|\omega|^{1/3}\mathrm{sign}(\omega)$ for small variations of the field angle near $\pi/6$. This is analogous to the non-linear susceptibility of the Ising ferromagnet at criticality. A priori thermal fluctuations will renormalize this exponent to that of the 3d Ising model – there we have $\psi \sim |\omega|^{1/\delta}$ and the true value is approximately $\delta \approx 4.8$.

One can readily calculate the torque $\tau = df/d\theta$, where the total derivative should be taken with respect to the field angle of the energy optimized at $\phi = \phi(\theta)$. Using the energy minimization condition, one obtains $\tau = 2uh\sin(\phi(\theta) + \theta)$, which is plotted in Fig. 3. It is

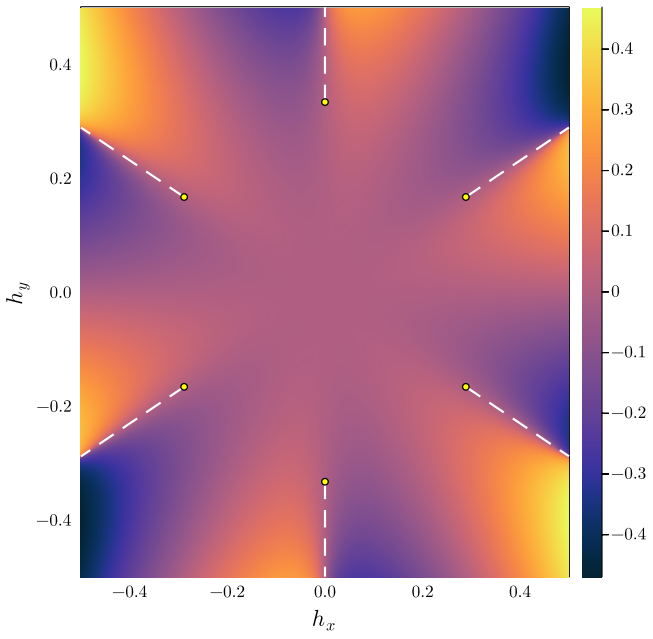

FIG. 3. Density plot of torque (τ/u) versus in-plane magnetic field. The field scale is chosen so that $h_c = 1/3$. Yellow circles mark the location of Ising critical points, and the first order lines are marked with dashed lines.

discontinuous across the first order transition lines, and vanishes when θ is a multiple of $\pi/3$.

The angular transition may also be detectable by means other than the torque. Hysteresis may occur and domains may form near the first order lines. The spin angles themselves could be observed directly in neutron scattering. It is interesting to point out that a very similar phenomena has already been observed in CeAlGe, in which the spontaneous formation of domains was argued to give rise to a sharp peak in the resistance versus angle, dubbed singular angular magneto-resistance[21]. It would be very interesting to study the angular dependence of the resistance in Mn_3Sn in an appropriate range.

From the calculations in Ref.[20], and the Supplemental Material of Ref.[5], we can compare directly to Eq. (18), and extract the parameters of the symmetry based theory in terms of microscopics. In the classical zero temperature model, one obtains thereby

$$u = \frac{K}{J + \sqrt{3}D}, \qquad v = \frac{D}{3\sqrt{3}(J + \sqrt{3}D)^3}. \tag{22}$$

This leads to the critical field, restoring units

$$H_c = \frac{J + \sqrt{3}D}{g\mu_B}\sqrt{\frac{K}{D}}. \tag{23}$$

Taking $D = 0.2J$, $K = .006J$, $J = 20meV$ and $g = 3$ yields $H_c \approx 20T$. This is of course to be renormalized by thermal and quantum fluctuations, but gives an idea of the order of magnitude. It strongly suggests the transition should be within range of current experiments.

ACKNOWLEDGMENTS

I thank Kamran Behnia, Zengwei Zhu, and Xiaokang Li for the experimental collaboration that inspired this work. This research is supported by the NSF CMMT program under Grant No. DMR-2116515.

[1] M. Collins and O. Petrenko, Review/synthèse: Triangular antiferromagnets, Canadian journal of physics **75**, 605 (1997).
[2] O. A. Starykh, Unusual ordered phases of highly frustrated magnets: a review, Reports on Progress in Physics **78**, 052502 (2015).
[3] M. Elhajal, B. Canals, R. Sunyer, and C. Lacroix, Ordering in the pyrochlore antiferromagnet due to dzyaloshinsky-moriya interactions, Physical Review B **71**, 094420 (2005).
[4] S. Nakatsuji, N. Kiyohara, and T. Higo, Large anomalous hall effect in a non-collinear antiferromagnet at room temperature, Nature **527**, 212 (2015).
[5] X. Li, S. Jiang, Q. Meng, H. Zuo, Z. Zhu, L. Balents, and K. Behnia, The free energy of twisting spins in Mn_3Sn (2021), arXiv:2109.11122 [cond-mat.str-el].
[6] X. Li, C. Collignon, L. Xu, H. Zuo, A. Cavanna, U. Gennser, et al., Chiral domain walls of mn_3sn and their memory, Nat. Commun. **10**, 1 (2019).
[7] X. Li, L. Xu, H. Zuo, A. Subedi, Z. Zhu, and K. Behnia, Momentum-space and real-space berry curvatures in mn_3sn, SciPost Phys. **5**, 063 (2018).
[8] P. Park, J. Oh, K. Uhlířová, J. Jackson, A. Deák, L. Szunyogh, et al., Magnetic excitations in non-collinear antiferromagnetic weyl semimetal mn_3sn, npj Quantum Mater. **3**, 1 (2018).
[9] J. Cable, N. Wakabayashi, and P. Radhakrishna, Magnetic excitations in the triangular antiferromagnets mn_3sn and mn_3ge, Phys. Rev. B **48**, 6159 (1993).
[10] T. Nagamiya, S. Tomiyoshi, and Y. Yamaguchi, Triangular spin configuration and weak ferromagnetism of mn3sn and mn3ge, Solid State Communications **42**, 385 (1982).
[11] A. Zorko, M. Pregelj, M. Gomilšek, M. Klanjšek, O. Zaharko, W. Sun, and J.-X. Mi, Negative-vector-chirality 120° spin structure in the defect- and distortion-free quantum kagome antiferromagnet $ycu_3(OH)_6cl_3$, Phys. Rev. B **100**, 144420 (2019).
[12] R. Okuma, T. Yajima, D. Nishio-Hamane, T. Okubo, and Z. Hiroi, Weak ferromagnetic order breaking the threefold rotational symmetry of the underlying kagome lattice in $CdCu_3(OH)_6(NO_3)_2 \cdot h_2O$, Phys. Rev. B **95**, 094427 (2017).
[13] Y. Ihara, H. Yoshida, K. Arashima, M. Hirata, and T. Sasaki, Anisotropic magnetic excitations from single-chirality antiferromagnetic state in ca-kapellasite, Phys. Rev. Research **2**, 023269 (2020).

[14] K. Iida, H. K. Yoshida, A. Nakao, H. O. Jeschke, Y. Iqbal, K. Nakajima, S. Ohira-Kawamura, K. Munakata, Y. Inamura, N. Murai, M. Ishikado, R. Kumai, T. Okada, M. Oda, K. Kakurai, and M. Matsuda, $q = 0$ long-range magnetic order in centennialite $\mathrm{cacu_3(OD)_6cl_2{\cdot}0.6d_2O}$: A spin-$\frac{1}{2}$ perfect kagome antiferromagnet with $J_1 - J_2 - J_d$, Phys. Rev. B **101**, 220408 (2020).

[15] R. Chen, H. Ju, H.-C. Jiang, O. A. Starykh, and L. Balents, Ground states of spin-$\frac{1}{2}$ triangular antiferromagnets in a magnetic field, Phys. Rev. B **87**, 165123 (2013).

[16] M. E. Zhitomirsky, Magnetic phase diagram of a partially frustrated triangular antiferromagnet: The row model, Phys. Rev. B **54**, 353 (1996).

[17] A. Chubukov and D. Golosov, Quantum theory of an antiferromagnet on a triangular lattice in a magnetic field, Journal of Physics: Condensed Matter **3**, 69 (1991).

[18] M. Gvozdikova, P. Melchy, and M. Zhitomirsky, Magnetic phase diagrams of classical triangular and kagome antiferromagnets, Journal of Physics: Condensed Matter **23**, 164209 (2011).

[19] Explicitly $\mathsf{O}_3 = \begin{pmatrix} \cos\frac{2\pi}{3} & \sin\frac{2\pi}{3} & 0 \\ -\sin\frac{2\pi}{3} & \cos\frac{2\pi}{3} & 0 \\ 0 & 0 & 1 \end{pmatrix}$.

[20] J. Liu and L. Balents, Anomalous Hall effect and topological defects in antiferromagnetic Weyl semimetals: $\mathrm{Mn_3Sn/Ge}$, Phys. Rev. Lett. **119**, 087202 (2017).

[21] T. Suzuki, L. Savary, J.-P. Liu, J. W. Lynn, L. Balents, and J. G. Checkelsky, Singular angular magnetoresistance in a magnetic nodal semimetal, Science **365**, 377 (2019), https://science.sciencemag.org/content/365/6451/377.full.pdf.